



CORRELATION BETWEEN STRUCTURE-SPECIFIC INTENSITY MEASURES OF SITE-DEPENDENT MOTIONS AND FRAME RESPONSE

I.K. Fontara⁽¹⁾, K. Kostinakis⁽²⁾, A. Athanatopoulou⁽³⁾

⁽¹⁾ Post-doctoral researcher, Department of Civil Engineering, Technical University of Berlin, Germany, fontara@tu-berlin.de

⁽²⁾ Post-doctoral researcher, Department of Civil Engineering, Aristotle University of Thessaloniki, Greece, kkostina@civil.auth.gr

⁽³⁾ Professor, Department of Civil Engineering, Aristotle University of Thessaloniki, Greece, minak@civil.auth.gr

Abstract

The assessment of the seismic performance of a structure depends on the optimal choice of an earthquake Intensity Measure (IM). Given the fact that conventional IMs based only on ground motion information might not be able to successfully predict the seismic response of structures, several advanced structure-specific IMs have been proposed during the past years, taking into account not only earthquake characteristics but also structural information. Moreover, local site conditions may generate large amplifications as well as spatial variations in the ground motions, which influence the intensity measures and in most cases lead to important structural damage.

Along these lines the objective of this paper is to study the correlation between well-known structure-specific intensity measures and the inelastic response of multi-story reinforced concrete planar frames taking into account site effects. First, site dependent ground motions are produced considering 2D analysis of the soil profile via Boundary Element Method (BEM) numerical technique. Three different geological configurations are considered that account for (i) uniform excitation, ii) canyon topography and iii) complex hills topography. Next, we focus on the dynamic behavior of two reinforced concrete frames (a symmetric and an asymmetric one) modeled and analyzed by the Finite Element Method (FEM). The buildings are subjected to a set of site-dependent strong motions and the expected structural damage state of each building is determined in terms of the Maximum Interstory Drift Ratio (MIDR). Then, a number of structure-specific seismic intensity measures is computed from the aforementioned site-dependent ground motions. The examined intensity measures take into account special characteristics of both the earthquake record and the building under consideration. The values of the MIDRs are correlated with the structure-specific ground motion intensity measures. In sum, the numerical results of this study show that certain intensity measures exhibit strong correlation with the seismic damage of the two buildings. However, their adequacy for estimation of structural response depends strongly on the local site conditions under investigation.

Keywords: structure-specific intensity measures; site effects; boundary element method; r/c buildings; non-linear response



1. Introduction

The basic concept of Performance-Based Seismic Design is to estimate the mean annual frequency of exceeding specified limit states for a given structure and site. In order to estimate this frequency, it is necessary to introduce two intermediate variables, one describing the structural demand and the other describing the ground motion Intensity Measure (IM) for the site under investigation. A successful correlation of the aforementioned variables leads to more accurate evaluation of seismic performance.

Given the fact that conventional IMs based only on ground motion information might not be able to successfully predict the seismic response of structures, several advanced structural-specific IMs have been proposed during the past years, taking into account not only earthquake characteristics but also structural information. Many researchers introduced scalar structure-specific IMs and they investigated their ability to predict the structural performance (e.g. [1-3]). They found that the structure specific IMs can adequately predict the seismic response of planar bending frames. Fontara et al. [4] examined the correlation between a number of advanced, structure-specific ground motion IMs and the structural damage of multistory R/C regular and irregular planar frames. It was shown that the IMs which take into consideration the effects of inelastic behavior through the spectral shape indicate the strongest correlation with the structural damage for low as well as high nonlinear response. Moreover, the adequacy of several advanced IMs was also examined by Kostinakis et al. [5-8] in the prediction of the structural damage of 3D buildings designed with the aid of modern seismic codes. It was demonstrated that the efficiency of the IMs depends on the selected engineering demand parameter evaluating the structural response as well as on the special building's characteristics. A preliminary ranking of alternative scalar structure-specific IMs was also carried out by Ebrahimian et al. [9]. Sets of suitable IMs were produced based on both efficiency and sufficiency criteria for different type of base fixities as well as different type of ground motions (i.e. ordinary and pulse-like).

Ground motion intensity measures are computed from strong motions recorded at a given site. Experience from previous earthquakes has shown that the intensity of ground shaking and earthquake damage is strongly influenced by local site conditions. Actual conditions at strong motion recording sites are highly variable with respect to local geotechnical condition. Therefore, an optimal seismic intensity measure should contain information about the ground motion, the local site conditions and the structure under investigation. However, none of the above mentioned investigations have taken into consideration the influence of local site condition in the evaluation of the IMs.

The objective of the present paper is to investigate the correlation between well-known structure-specific seismic IMs and the inelastic response of multi story reinforced concrete planar buildings taking into account site effects. First, site dependent ground motions are produced considering 2D analysis of the soil profile via the BEM numerical technique. Several complex geological configurations that account for hill and canyon effects are taken into consideration. Next, two reinforced concrete frames are subjected to the set of the site-dependent strong motions. For each earthquake record the expected structural damage state of each building is determined and correlated with the values of several structure-specific intensity measures.

2. Ground motions

2.1 Seismic signal recovering methodology

There is a lack of high performance computational tools able to simulate 2D and possibly 3D complex unbounded geological media. Among the numerical methods the BEM is recognized as a valuable technique to solve wave propagation problems due to many advantages in comparison with other domain techniques such as the FEM. It is briefly mentioned herein that it is possible to deal with infinite or semi-infinite media with high accuracy and minimal modeling effort due to implicit satisfaction of the radiation condition associated with unbounded domains.

In the present study, the BEM is used to model the seismic wave propagation through complex geological profiles so as to recover ground motion records that account for local site conditions. In particular consider 2D wave propagation in viscoelastic, isotropic half-plane consisting of N parallel or non-parallel inhomogeneous

layers Ω_n ($n=0,1,2,\dots,N$) with a free surface and sub-surface relief of arbitrary shape. The dynamic disturbance is provided by either an incident SH wave or by waves radiating from an embedded seismic source, see Fig.1. The BEM numerical scheme employed here was developed and validated in Fontara [10] and we briefly present its formulation in what follows.

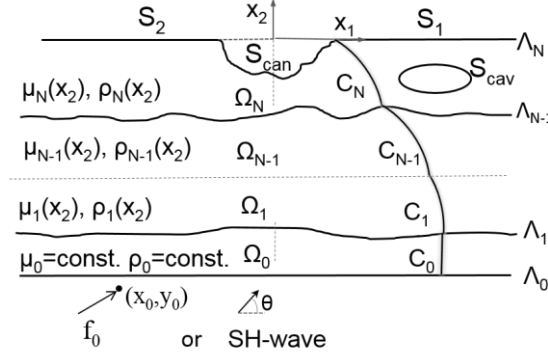


Fig. 1 – Geometry of the problem treated by BEM: A multilayer geological medium with surface topography and buried inclusions.

For this problem a half-plane consisting of two homogeneous layers and surface relief of arbitrary shape under incident SH wave is analyzed. For the formulation of the boundary integral equation we use the well-known boundary integral representation formula and insert as kernels the fundamental solutions for homogeneous full plane [11]:

$$cu_3^{(i)}(\mathbf{x}, \omega) = \int_{\Gamma} U_3^{*(i)}(\mathbf{x}, \mathbf{y}, \omega) t_3^{(i)}(\mathbf{y}, \omega) d\Gamma - \int_{\Gamma} P_3^{*(i)}(\mathbf{x}, \mathbf{y}, \omega) u_3^{(i)}(\mathbf{y}, \omega) d\Gamma \quad (1)$$

$$\mathbf{x} \in \Gamma = \Omega_i \cup S_{can} \cup S_{cav}$$

In Eq. (1), \mathbf{x} , \mathbf{y} are source and field points, respectively, c is the jump term, U_3^* is the fundamental solution for homogeneous full-plane, and $P_3^*(\mathbf{x}, \mathbf{y}, \omega) = \mu(\mathbf{x}) U_3^*(\mathbf{x}, \mathbf{y}, \omega) n_i(\mathbf{x})$ is the corresponding traction fundamental solution, where $i=1, 2, \dots, N$ is the number of layers. The above equation is written in terms of total wave field and expresses the case of incident SH waves. Note that only the layer interfaces, as well as the free and sub-surface relief are discretized. After discretization of all boundaries with constant (i.e., single node) boundary elements, the matrix equation system is formed below and displacements along the free surface can be computed:

$$[\mathbf{G}]\{\mathbf{t}\} - [\mathbf{H}]\{\mathbf{u}\} = \{\mathbf{0}\} \quad (2)$$

The above system matrices \mathbf{G} and \mathbf{H} result from numerical integration using Gaussian quadrature of all surface integrals containing the products of fundamental solutions times interpolation functions used for representing the field variables. They are fully populated matrices of size $N \times N$, where N is the total number of nodes used in the discretization of all surfaces and interfaces, while vectors u and t now contain the nodal values of displacements and tractions at all boundaries. Finally, the generation of transient signals from the hitherto derived time-harmonic displacements is achieved through inverse Fourier transformation. The aforementioned BEM numerical implementation and production of the final seismic signal is programmed using the Matlab software package.

2.2 Geological profiles

The methodology described in the previous section is now applied to three different hypothetical geological profiles on which the investigated structures are considered to be located, see Fig.2 below. The examined geological key parameters are the canyon topography and the complex hills topography.

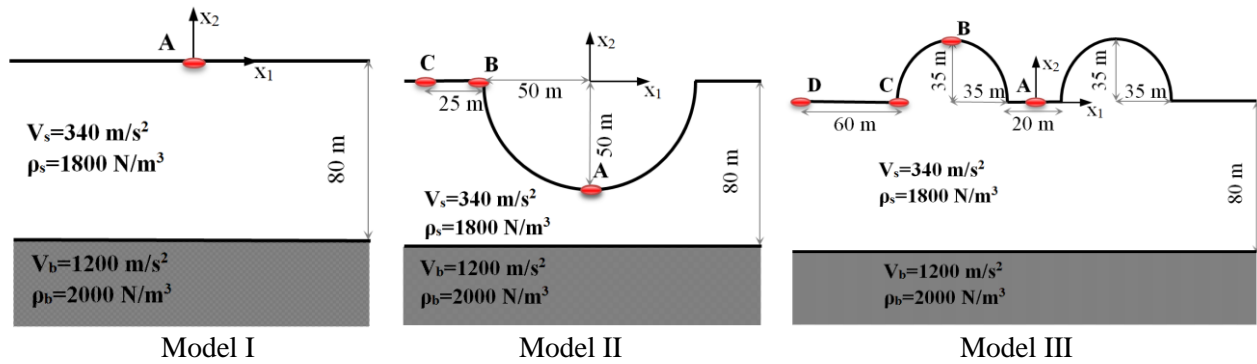


Fig. 2 – Three geological profiles, namely Model I-III and receiver points A, B, C and D on which the structures are assumed to be located.

In particular, the site is represented by the following geological profiles: (I) a homogeneous layer with flat free surface producing a uniform excitation at the free surface; (II) a homogeneous layer with a valley in which the structures are considered to be located at different points along the canyon A, B and C; (III) a homogeneous layer with two hills in which the structures are considered to be located at different points along the free surface A, B, C and D. All geological profiles are overlying bedrock. All geological configurations have the same material properties and are shown in Fig.2. A suite of thirty earthquake excitations given in Table 1 are recorded at the outcropping rock on site class A (according to FEMA classifications) and are drawn from the PEER [12] strong motion database. These records are considered as an input at the seismic bed level for all geological profiles.

Table 1 – Data of earthquake records

No	Date	Earthquake name	Moment Magnitude (M_w)	Station name	Closest distance (Km)	PGA (g) (uncorrelated)	Component (deg)
1	9/2/1971	San Fernando	6.61	Cedar Springs	89.4	0.020	95
2	9/2/1971	San Fernando	6.61	Pasadena	21.5	0.205	180
3	18/10/1989	Loma Prieta	6.93	Piedmont Jr	73.0	0.099	315
4	18/10/1989	Loma Prieta	6.93	Point Bonita	83.5	0.076	207
5	18/10/1989	Loma Prieta	6.93	Pacific Height	76.1	0.070	270
6	18/10/1989	Loma Prieta	6.93	Rincon Hill	74.1	0.102	0
7	18/10/1989	Loma Prieta	6.93	Sierra Pt.	63.2	0.110	115
8	17/1/1994	Northridge	6.69	Wonderland	20.3	0.160	95
9	17/1/1994	Northridge	6.69	Vasquez Park	23.6	0.152	0
10	20/9/1999	Chi-Chi	7.62	CHY102	37.7	0.048	E
11	20/9/1999	Chi-Chi	7.62	HWA003	56.1	0.138	N
12	20/9/1999	Chi-Chi	7.62	KAU034	108.6	0.011	E
13	20/9/1999	Chi-Chi	7.62	KAU042	160.2	0.011	E
14	20/9/1999	Chi-Chi	7.62	KAU051	125.2	0.010	E
15	20/9/1999	Chi-Chi	7.62	TAP046	118.3	0.079	E
16	20/9/1999	Chi-Chi	7.62	TAP065	122.5	0.041	E
17	20/9/1999	Chi-Chi	6.2	TCU085	103.6	0.005	E
18	20/9/1999	Chi-Chi	6.2	TTN042	93.6	0.011	N
19	20/9/1999	Chi-Chi	6.2	CHY102	39.3	0.058	E
20	20/9/1999	Chi-Chi	6.2	KAU003	116.2	0.011	N
21	20/9/1999	Chi-Chi	6.2	TTN042	69.0	0.029	N
22	22/9/1999	Chi-Chi	6.2	CHY102	74.2	0.068	E
23	22/9/1999	Chi-Chi	6.2	HWA003	50.4	0.033	N
24	22/9/1999	Chi-Chi	6.2	ILA001	134.9	0.008	N
25	22/9/1999	Chi-Chi	6.2	KAU051	159.5	0.007	E
26	22/9/1999	Chi-Chi	6.2	TAP067	131.5	0.010	E
27	22/9/1999	Chi-Chi	6.2	TAP075	142.9	0.013	N
28	22/9/1999	Chi-Chi	6.2	TAP077	152.1	0.009	N
29	22/9/1999	Chi-Chi	6.2	TAP086	128.2	0.020	E
30	22/9/1999	Chi-Chi	6.2	TCU085	91.8	0.015	E

2.3 Site dependent ground motions

Next, we investigate the influence of canyon topography as well as complex hills topography on ground motions recorded along the free surface. Consider the first geological profile (Model I), comprising a single layer with horizontal free surface resting over bedrock that produces uniform excitation, as reference case. Fig.3 plots the mean value of the 30 acceleration response spectra produced from the ground motions recorded at different points A, B, C and D at the free surface of Model I, II and III. The shape of the response spectra is modified as the geological profile becomes more complex. This is also evident from the 3D time history of Loma Prieta No7 ground motion generated along the free surface of (a) Model I, (b) Model II and (c) Model III geological profile shown in Fig.4. The seismic signal depends strongly on the presence of free surface relief like canyon or hill topography. From Fig.3 we observe that spectral acceleration values can differ significantly when they are recorded at different points along the surface topography. Seismic signals recorded at the edge of the canyon or hill (point B, Model II and Model III) are more pronounced due to wave scattering phenomena occurring at complex surface topographies.

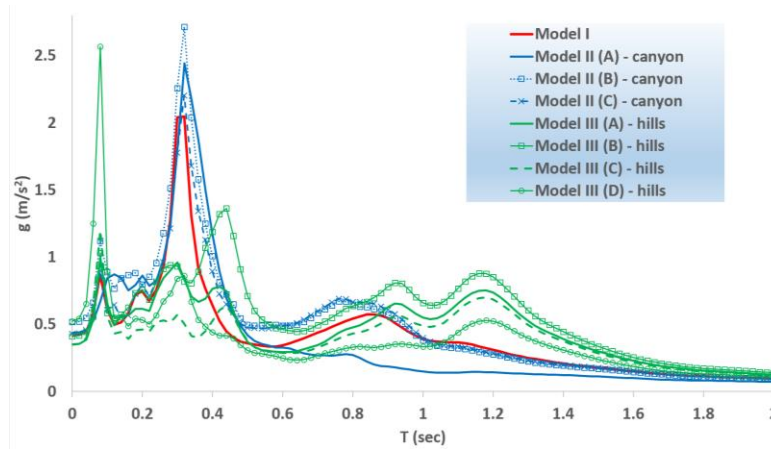


Fig. 3 – Mean value of the 30 acceleration response spectra produced from the ground motions recorded at different receiver points A, B, C and D at the free surface of Model I, II and III.

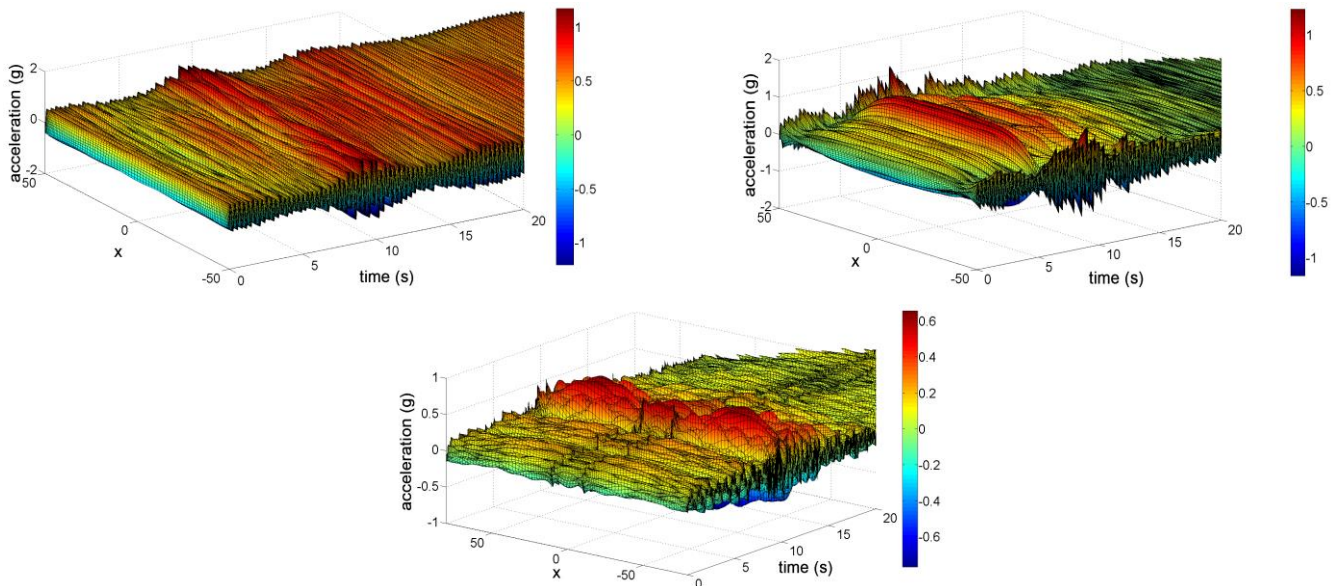


Fig. 4 – 3D acceleration time-history of Loma Prieta No7 ground motion recorded along the free surface of (a) Model I, (b) Model II and (c) Model III geological profile.

0.5% < MIDR < 1.0% and 3) heavy for MIDR > 1.0%. The number of records which cause slight, moderate and heavy damage in the examined buildings are shown in Fig.6.

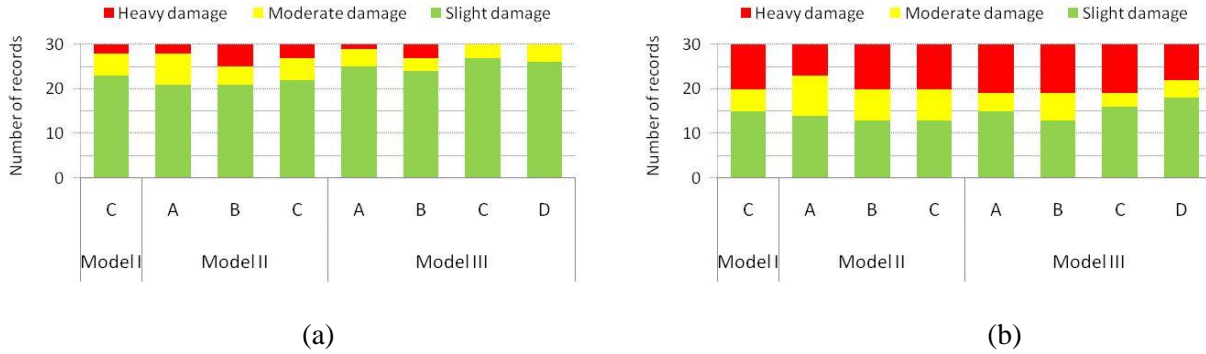


Fig. 6 – Number of records corresponding to each damage degree for the 3-story (a) and the 7-story (b) building.

4. Intensity measures

In the present paper the evaluated ground motion intensity measures are determined via eigenvalue analyses. The examined IMs were proposed by researchers in an attempt to avoid the major shortcomings associated with $S_a(T_1)$; namely, ignoring both the contribution of higher modes to the overall dynamic response and the increase of the fundamental period of the structure (period elongation) associated with non-linear behavior. More specifically, the following advanced, structure-specific IMs are considered:

- IM proposed by Cordova et al. [1] ($IM_{Cordova\ et\ al}$).

$$IM_{Cordova\ et\ al} = S_a(T_1) \cdot \left[\frac{S_a(2T_1)}{S_a(T_1)} \right]^{0.5} \quad (3)$$

- IM proposed by Luco [17] and Luco and Cornell [2] ($IM_{Luco\ \&\ Cor}$).

$$IM_{Luco\ \&\ Cor} = \sqrt{(\Gamma_1 \cdot ID_1 \cdot S_d(T_1))^2 + (\Gamma_2 \cdot ID_2 \cdot S_d(T_2))^2} \quad (4)$$

where Γ_1 and Γ_2 are the 1st and 2nd-mode participation factors respectively, ID_1 and ID_2 are the 1st and 2nd-mode interstorey drifts that correspond to the story at which the quantity under the square root is maximized.

- IM proposed by Yahyaabadi and Tehranizadeh [3] for Non-Collapse seismic demand prediction ($IM_{Yah\ \&\ Tehr, NC}$).

$$IM_{Yah\ \&\ Tehr, NC} = \left[0.8S_d^2(T_1) + 0.2S_d^2(1.2T_1) \right]^{0.5} \quad (5)$$

where $S_d(T_1)$ is the spectral displacement for the first mode period of the structure.

- IM proposed by Yahyaabadi and Tehranizadeh [3] for Collapse seismic demand prediction ($IM_{Yah\ \&\ Tehr, C}$).

$$IM_{Yah\ \&\ Tehr, C} = \left[0.4S_d^2(T_1) + 0.4S_d^2(1.2T_1) + 0.2S_d^2(1.6T_1) \right]^{0.5} \quad (6)$$



- IM proposed by Lin et al. [18] ($IM_{Lin\ et\ al}$).

$$IM_{Lin\ et\ al} = S_a(T_1)^{0.5} \cdot S_a(1.5T_1)^{0.5} \quad (7)$$

- IM proposed by Kappos [19] (IM_{Kappos}).

$$IM_{Kappos} = \int_{T_{1-t}}^{T_{1+t}} S_v(T, \xi) dT \quad (8)$$

where S_v is the spectrum velocity curve and $t=0.2T_1$.

- IM proposed by Bojorquez & Iervolino [20] ($IM_{Boj\ \&\ Ier}$).

$$IM_{Boj\ \&\ Ier} = S_a(T_1) \cdot \left[\frac{GMV(S_a(T_1...2T_1))}{S_a(T_1)} \right]^{0.4} \quad (9)$$

where $GMV(S_a(T_1)..S_a(2T_1))$ is Geometric Mean Value of the spectral acceleration over a range of periods between T_1 and $2T_1$.

5. Correlation study of the results

In order to evaluate the relative adequacy of the examined IMs for the various site dependent ground motions, the correlation between the intensity measures corresponding to each ground motion and the produced MIDR, is computed using the Pearson correlation coefficient (Eq. (10)). The Pearson correlation coefficient shows how well the data fit a linear relationship and ranges between -1 and 1.

$$p = \frac{\sum_{i=1}^N (X_i - \bar{X}) \cdot (Y_i - \bar{Y})}{\sqrt{\sum_{i=1}^N (X_i - \bar{X})^2 \cdot \sum_{i=1}^N (Y_i - \bar{Y})^2}} \quad (10)$$

where: \bar{X} and \bar{Y} are the mean values of X_i and Y_i data respectively and N is the number of pairs of values X_i, Y_i in the data.

The Pearson's correlation coefficients between the examined IMs and the MIDR of the two buildings are shown in Fig.7. The figure illustrates the results produced for the three geological profiles, as well as for the four different points at the free surface considered in the present study. The general observation, which can be made is that, considering the 3-story building, the correlation between the IMs and the seismic damage depends on the site effects. However, the influence of the site effects on the correlation coefficients is weaker in case of the 7-story structure.

Regarding the 3-story building, from Fig.7(a) it can be seen that the IMs exhibit weaker correlation with structural damage for geological model III compared with model I and II. The correlation between structural damage and the IMs is weaker as the considered geological profile becomes more complex and subsequently the influence of site effects is greater. The presence of local site effects can lead to 65% difference on the correlation degree of a certain IM with the structural damage. Observe that a given IM computed at different points along

the canyon or hill surface topography produce different correlation coefficients with the structural damage. For example, observe that Pearson's correlation coefficient between seismic damage and the IM proposed by Kappos [19] attains the values of 0.35 and 0.85 when the calculation is made considering points B and D of Model III respectively.

Another observation of significant importance made from Fig.7 is that the relative adequacy of the examined IMs is strongly affected by the presence of local site conditions. Observe that the IM proposed by Cordova et al. [1] demonstrates the highest and the most robust correlation capacity for all geological profiles considered. Note that $IM_{Cordova\ et\ al}$ attains values greater than 0.8 for all cases with exception of Point B Modell III where it drops to 0.58. Regarding the other IMs examined in the present study, we can see that the IMs introduced by Yahyaabadi and Tehranizadeh [3] (for Collapse as well as for Non-Collapse seismic demand prediction) and by Bojorquez & Iervolino [20] exhibit strong enough correlation with the structural damage of the building. The IMs that lead to the poorest correlation with the seismic damage are the ones proposed by Kappos [19] and Luco and Cornell [2].

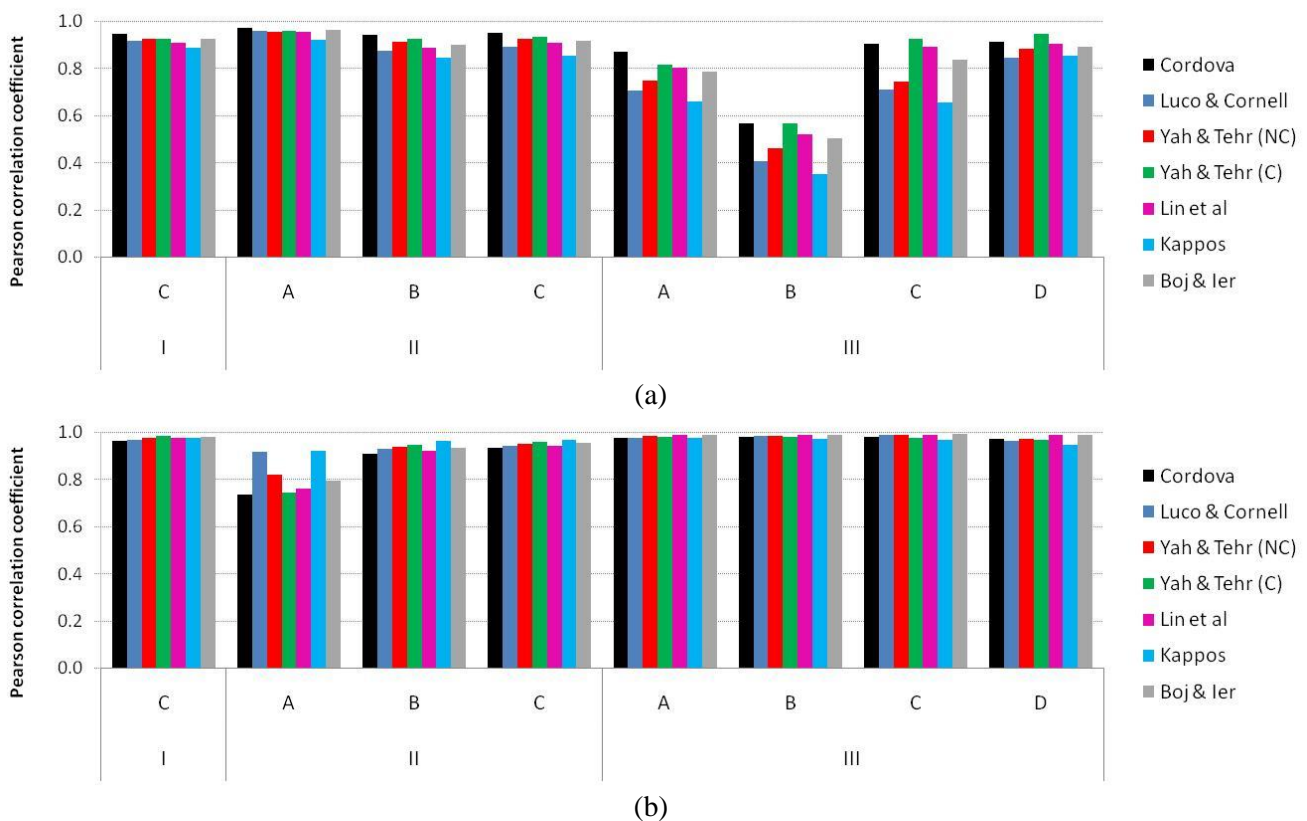


Fig. 7 – Pearson's correlation coefficients between the IMs and MIDR of the 3-story (a) and the 7-story (b) building for the three geological profiles.

From Fig.7(b) we can see that all examined IMs can correlate efficiently with the structural damage in case of the 7-story frame. All IMs are stable against the presence of local site conditions. The 7-story frame produces high nonlinear behavior under the investigated site-dependent ground motions as shown in Fig.6. Given the fact that nonlinear behavior results on period elongations, then for $T > 1.2s$ the influence of site effects is small according to the site dependent response spectra shown in Fig.3. An exception to this is the case study of Model II and point A, where the frame exhibits slight to moderate damage for the most input motions and consequently expresses great influence of the presence of site effects. For this case the IM proposed by Kappos [19] produced the highest correlation and the IM introduced by Cordova et al. [1] led to the poorest correlation ($p=0.74$), result that contradicts the outcome reached for the case of stiffer 3-story frame.

In order to generalize trends, the results for the three geological profiles and the four points at the free surface were ranked in Fig.8 in order to choose the IM with the best global correlation to damage levels. Note

that small values of the ranks for a certain IM denote high correlation between the IM and the seismic damage. From Fig.8(a) we can see that, in case of the 3-story building, the strongest correlation is produced when the $IM_{Cordova\ et\ al}$ and $IM_{Yah\ \&\ Tehr,\ C}$ are adopted, with the IM proposed by Bojorquez & Iervolino [20] following. Regarding the IMs that led to the poorest correlation with the seismic damage, then we can see that these are the ones proposed by Kappos [19] and Luco and Cornell [2]. It must be noticed that the above conclusions are in agreement with the ones presented in Fig.7(a). Concerning the 7-story building, Fig.8(b) reveals that, as mentioned above, the sum of the ranks for the examined IMs do not show significant differences, revealing that the relative adequacy of the seven IMs is almost the same. As an exception, we can mention the IM proposed by Cordova et al. [1], which seems to produce the weakest correlation in most cases.

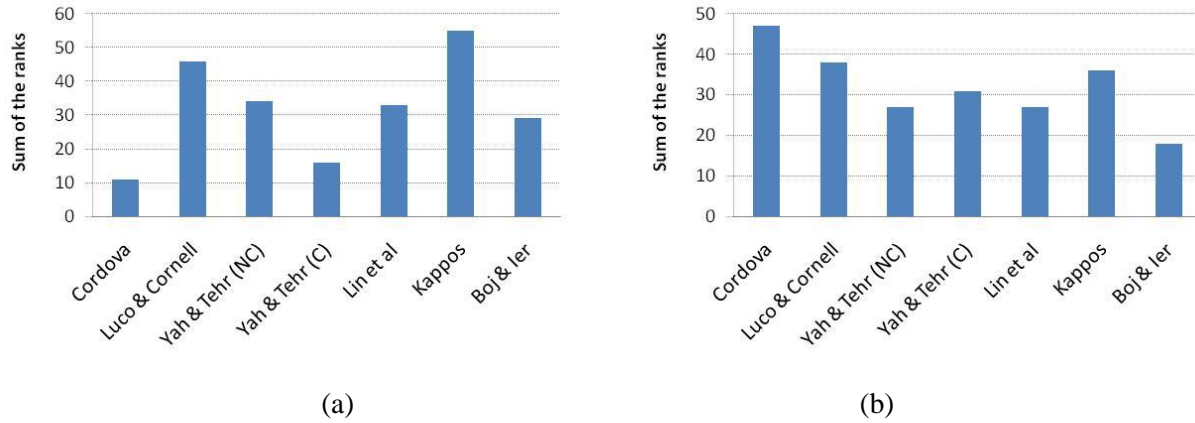


Fig. 8 – Sum of the ranks over the three geological profiles and the four points at the free surface in case of the 3-story (a) and the 7-story (b) building

Furthermore, the results for the seven examined IMs were ranked to choose the geological profile with the best global correlation to damage levels. The Fig.9 illustrates the results. From this figure we can see that, in case of the 3-story building (Fig.9(a)), the strongest correlation is produced for models I and II and the weakest for model III. Comparing the results obtained for the four different points of the free surface, we can see that for model II and III the poorest correlation is demonstrated for point B (edge of the canyon). Concerning the 7-story building, Fig.9(b) reveals that the correlation between seismic damage and the IMs is stronger in case of models I and III and weaker for model II, since input motions produced from Model I and III induce high nonlinearity in the 7-story structure. Note that the above conclusions agree with the ones presented above.

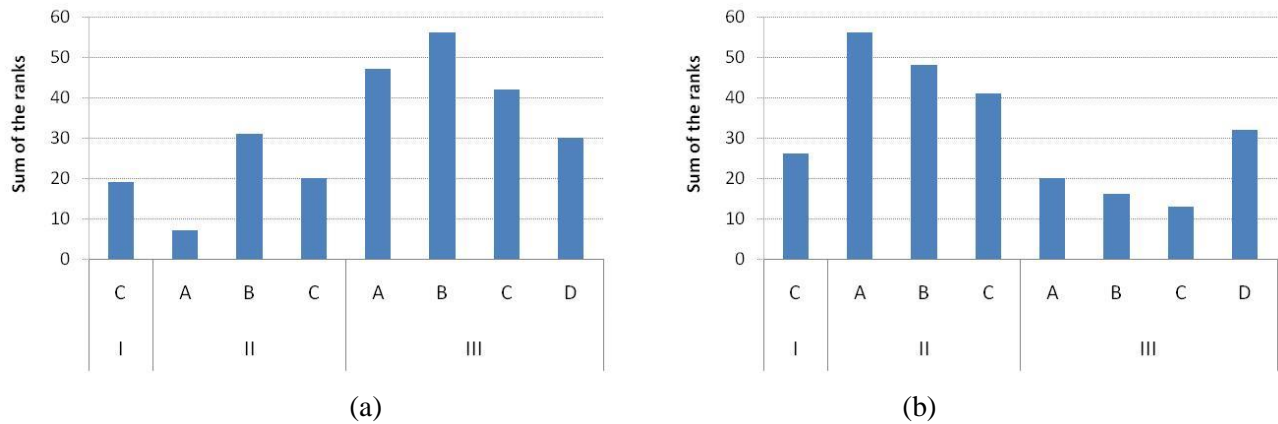


Fig. 9 – Sum of the ranks over the seven examined IMs in case of the 3-story (a) and the 7-story (b) building

6. Conclusions

The present study investigates the correlation between well-known structure-specific seismic IMs and the



inelastic response of multi story reinforced concrete planar buildings taking into account site effects. As a first step, site dependent ground motions are produced considering 2D analysis of the soil profile via the BEM numerical technique. Several complex geological configurations that account for canyon and complex hill surface topography are considered. Next, two reinforced concrete frames are subjected to the set of the site-dependent strong motions. For each earthquake record the expected structural damage state of each building is determined and correlated with the values of many known structure-specific seismic intensity measures. The comparative assessment of the results has led to the following conclusions:

- Local site conditions may significantly influence the efficiency of the IMs used for the assessment of the seismic performance of structures. This influence is more pronounced for stiff and irregular buildings. Ignoring the case of local site conditions may lead to 65% difference on the correlation efficiency of a given IM.
- The IMs that take into consideration the effects of inelasticity through the acceleration or displacement spectral shape are shown to be the best predictors for the structural damage of medium rise stiff buildings taking into account local site conditions.
- All the examined IMs can correlate efficiently with the structural damage in case of soft buildings. Moreover, they are stable against the presence of local site conditions. This conclusion can be attributed to the fact that the 7-story frame examined in the present study produced high nonlinear behavior under the investigated site-dependent ground motions. Given the fact that nonlinear behavior results on period elongations, then the influence of site effects is small according to the site dependent response spectra of the strong motions.
- Ground motions recorded at the edge of the surface topography lead to significant amplifications in the ground motions that result on a great loss of the efficiency of IMs to predict the structural damage.

It must be noted that the aforementioned conclusions are valid for the investigated R/C frames, which have been designed with the aid of modern seismic codes.

7. References

- [1] Cordova PP, Deierlein GG, Mehanny SSF, Cornell CA (2001): Development of a two-parameter seismic intensity measure and probabilistic assessment procedure. *2nd US-Japan workshop on performance-based earthquake engineering methodology for RC building structures*, pp. 187-206.
- [2] Luco N, Cornell CA (2007): Structure-specific scalar intensity measures for near-source and ordinary earthquake motions. *Earthquake Spectra*, **23** (2), 357-392.
- [3] Yahyaabadi A, Tehranizadeh M (2011): New scalar intensity measure for near-fault ground motions based on the optimal combination of spectral response. *Scientia Iranica*, **18** (6), 1149-1158.
- [4] Fontara IK, Athanatopoulou A, Avramidis I (2012): Correlation between advanced, structure-specific ground motion intensity measures and damage indices. *15th World Conference on Earthquake Engineering*, Lisboa, Portugal.
- [5] Kostinakis K, Papadopoulos M, Athanatopoulou A (2014): Adequacy of advanced earthquake intensity measures for estimation of damage under seismic excitation with arbitrary orientation. *ICCSEE 2014: International Conference on Civil, Structural and Earthquake Engineering*, 28-29 April, Paris, France, Paper No: 214.
- [6] Kostinakis K, Papadopoulos M, Athanatopoulou A, Morfidis K (2014): Correlation between structure-specific ground motion intensity measures and seismic response of 3d R/C buildings. *2nd European Conference on Earthquake Engineering and Seismology*, 25-29 August, Instabul, Turkey.
- [7] Kostinakis K, Athanatopoulou A (2015): Prediction of seismic damage using scalar intensity measures based on integration of spectral values. *ICCSEE 2015: International Conference on Civil, Structural and Environmental Engineering*, 13-14 January, Zurich, Switzerland, Paper No: 113.
- [8] Kostinakis K, Athanatopoulou A (2015): Evaluation of scalar structure-specific ground motion intensity measures for seismic response prediction of earthquake resistant 3D buildings. *Earthquakes and Structures*, **9** (5), 1091-1114.



- [9] Ebrahimian H, Jalayer F, Lucchini A, Mollaioli F, Manfredi G (2015): Preliminary ranking of alternative scalar and vector intensity measures of ground shaking. *Bulletin of Earthquake Engineering*, **13** (10), 2805-2840.
- [10] Fontara I.K (2015): *Simulation of seismic wave fields in inhomogeneous half-plane by non-conventional BEM*, Christian-Albrechts-University in Kiel, Germany, 1, ISSN 2365-7162.
- [11] Dominguez J (1993): *Boundary Elements in Dynamics*. Computational Mechanics Publications, Southampton.
- [12] Pacific Earthquake Engineering Research Centre (PEER) (2003), Strong Motion Database. <http://peer.berkeley.edu/smcat/>.
- [13] CEN. Eurocode 8 (2003): *Design of structures for earthquake resistance - Part 1: General rules, seismic actions and rules for buildings*, European Committee for Standardization.
- [14] CEN. Eurocode 2 (2004): *Design of Concrete Structures, Part 1-1: General rules and rules for buildings*, European Committee for Standardization.
- [15] Otani A (1974): Inelastic Analysis of RC frame structures. *J Struct Div (ASCE)*, **100** (7), 1433-1449.
- [16] Naeim F (2001): *The seismic design handbook*, Kluwer Academic, Boston. 2nd Ed.
- [17] Luco N (2002): Probabilistic seismic demand analysis, SMRF connection fractures, and near-source effects. *Ph.D. thesis*, Department of Civil and Environmental Engineering, Stanford University, CA.
- [18] Lin L, Naumoski N, Saatcioglu M, Foo S (2011): Improved intensity measures for probabilistic seismic demand analysis. Part 1: development of improved intensity measures", *Canadian Journal of Civil Engineering*, **38**, 79-88.
- [19] Kappos AJ (1990): Sensitivity of calculated inelastic seismic response to input motion characteristics. *4th U.S. National Conference on Earthquake Engineering*, Palm Springs, California, 2:25-34.
- [20] Bojorquez E, Iervolino I (2011): Spectral shape proxies and nonlinear structural response. *Soil Dynamics and Earthquake Engineering*, **31**, 996-1008.